Aggregation of Thionine within AlMCM-48

Wei Xu, Metin Aydin, Sheuli Zakia, and Daniel L. Akins*

Center for Analysis of Structures and Interfaces (CASI), Department of Chemistry, The City College of The City University of New York, New York, New York 10031

Received: December 23, 2003; In Final Form: February 25, 2004

We report the formation of aggregated thionine molecules encapsulated within an Al-containing mesoporous molecular sieve material (specifically, AlMCM-48) that possesses a cubic pore structure. XRD, UV−vis absorption, fluorescence, and Raman measurements were used, where appropriate, as spectroscopic tools to characterize the AlMCM-48 host sample and the composite system consisting of the host and encapsulated thionine molecules. Due to the size of the cubic pores possessed by the host, aggregates of thionine larger than the dimers, trimers, and so forth, reported hitherto, are likely formed and are more appropriately termed H-aggregates. The structure of the H-aggregate is proposed. Raman band assignments for thionine are made based on both empirical determinations and quantum chemical calculations using density functional theory at the B3LYP level.

I. Introduction

Spectroscopic and optical dynamics properties of aggregated molecules in homogeneous systems (refs 1 and 2) and as adsorbates in heterogeneous systems (refs 3 and 14) have been extensively investigated in the authors' laboratory. Our interest derives principally from the fact that molecular aggregates have important current and potential technological applications, including as spectral sensitizers,[15] nonlinear optical materials,[16−20] and superradiant light emitters.[2]

The primary mechanism through which molecular aggregate structures are formed is self-assembly as a result of intrinsic intermolecular interactions. Often such self-assembled molecular structures can be classified as J- or H-aggregates, defined by the relative orientations of induced transition dipoles of the constituent molecules, either "head-to-tail" or "head-to-head," respectively.[21] Some of the more well-known molecules that have been identified as forming J- or H-aggregates include dyes such as the cyanines,[7−13,22−27] the xanthrenes,[28−30] the oxazines,[31] polycyclic aromatics,[32−37] and the porphyrins.[38−41] The structural picture suggested by the J- or H-aggregate designation often provides a framework for analysis of putative structural interactions and their impact on optical spectra and dynamics in aggregate systems. However the vast majority of aggregate systems that have been investigated have exhibited spectral properties associated with the J-aggregate, not the H-aggregate. Additionally, much research has focused on systems in which dyes have been encapsulated within various zeolites, particularly, L zeolite by Calzaferri et al.,[42] with the aim of developing light-harvesting antenna systems. In the present paper, we report studies dealing with a molecule that has been reported to form dimers and trimers and exhibits spectral properties that have led researchers to classify the small grouping of molecules as H-aggregates.[43,44] The particular molecule, thionine (see Chart 1), which is a characteristic thiazine dye, in the same family as methylene blue, in the present study is induced to enter the internal pores of AlMCM-48 by cation exchange between cationic thionine and (likely) cationic sodium sites within MCM-48 created by incorporation of Al within the silicate framework. Since the pore volume available to encapsulate thionine in AlMCM-48 is substantially greater than the pore volume available in zeolites (see ref 43) or the specific AOT reverse micelle system that has been used (see ref 44)—the latter, where dimer and trimer forms of thionine have been previously postulated to exist—one can anticipate that larger aggregated structures can be accommodated, resulting in a more traditional H-aggregate extended structure.

The AlMCM-48 molecular sieve material, which we synthesized for the present study, is compositionally identical to zeolites, but its pore structure is three-dimensional, uniform, and selectable during synthesis; however, the matrix is amorphous, not crystalline as in the zeolites. The pore size of the Al-containing MCM-48 that we synthesized was ascertained as having an average diameter of circa 27 Å, as indicated by nitrogen adsorption/desorption isotherm measurements.[45]

In the present work, we have studied the structural and optical properties of both solution phase monomeric thionine as well as thionine monomer and aggregate encapsulated within mesoporous AlMCM-48. Different spectroscopic measurements including X-ray diffraction (XRD), Raman scattering, UV−vis absorption, and fluorescence measurements have been utilized.

It is to be noted that for experimental systems such as those described herein, the most discerning technique for gaining structural information for aggregated molecules has proven to be that of Raman spectroscopy. The assignment of Raman bands for thionine, from earlier Raman investigations, has been empirical in nature.[46] However, theoretical approaches, including quantum mechanical methods, such as ab initio structural calculations and density functional theory (DFT),[47] can provide more informed insight concerning vibrational mode composition, optical dynamics, and other optical spectroscopic properties of thionine molecules. In the present paper, we utilize DFT to assign vibrational bands to specific motions of the thionine cation as well as assess the effect of aggregation on vibrational band shifts; we additionally interpret the magnitudes of such shifts in terms of the structure of the thionine aggregate. Charge density calculations are also utilized to gain insight on the extended structure of the aggregate.

10.1021/jp037994a CCC: $27.50
Published on Web 04/01/2004

CHART 1: Optimized Isolated Single Molecular Structure and Atomic Labeling with Averaged Bond Distances and Bond Angles

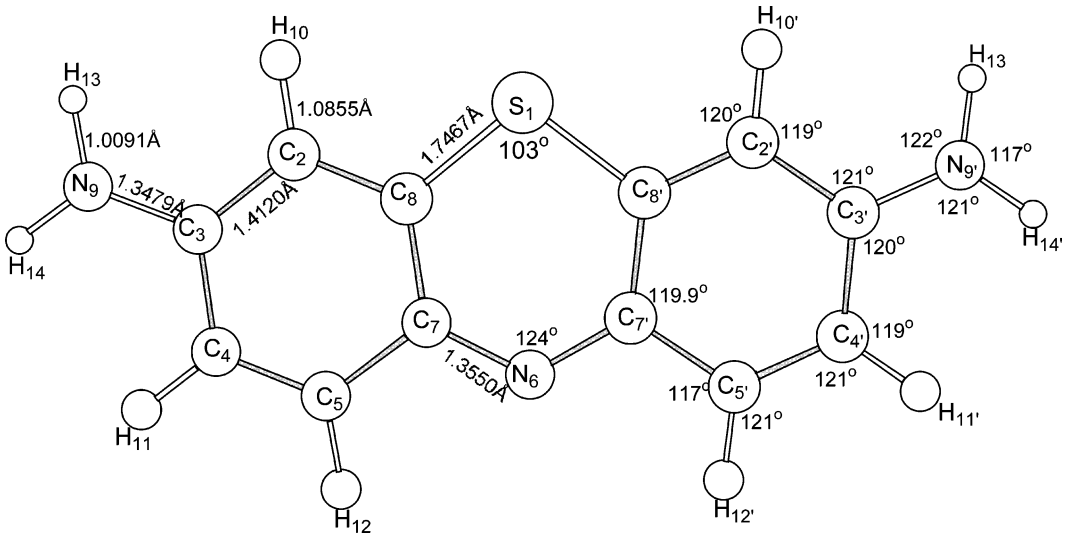

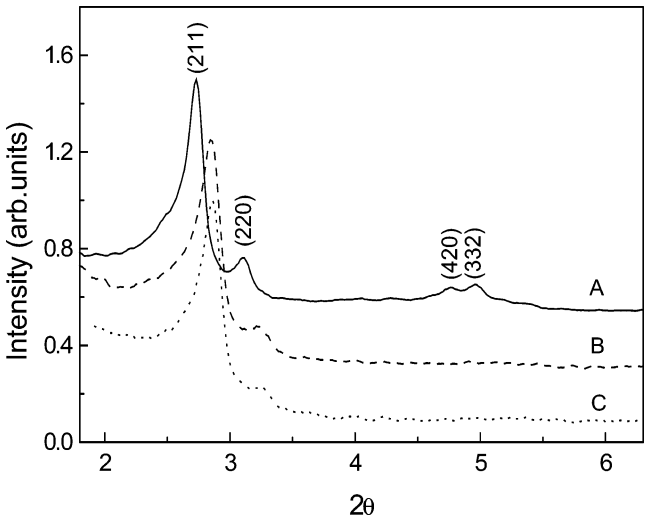

Figure 1. XRD patterns of (A) siliceous SiMCM-48 (solid line), (B) aluminum-containing AlMCM-48 (dashed line), and (C) H-aggregated composite thionine/AlMCM-48 (dotted line). The spacings between the d_{211} planes in A, B and C, respectively, are calculated as being ca. 3.2, 3.1, and 3.1 nm.

II. Experimental Section

A. Synthesis of Siliceous MCM-48 and Aluminum-Containing AlMCM-48. MCM-48 was synthesized by a method reported in the literature.[48] Briefly, a mixture containing 1.0 mol of tetraethyl orthosilicate (TEOS; Aldrich) and 0.5 mol of KOH in 62 mol of H_2O was stirred for 20 min at room temperature. Then 0.65 mol of cetyltetramethylammonium bromide (CTAB) was slowly added to the solution with stirring. After an additional 15 min of vigorous stirring, the temperature was raised to 388 K, and the reaction allowed to proceed for 48 h in a Teflon-lined autoclave. The resultant precipitate was filtered, washed thoroughly with warm distilled water, and then calcined in air at 773 K to obtain the siliceous product, MCM-48 (see Figure 1 for the XRD patterns). The granular MCM-48 white powder was used as the parent material to produce the aluminum-containing material, AlMCM-48.

The incorporation of aluminum within the silicate framework was undertaken in order to increase the quantity of positively charged monomeric thionine dye that might be encapsulated, due to guest−host intermolecular and/or electrostatic interactions within the porous material, thus promoting the formation of a molecular H-type aggregate that contains more than the 2 or 3 molecules (i.e., dimer or trimer, respectively) reported in the literature.[42−44]

For our studies, the aluminum-containing AlMCM-48 was prepared by using an approach similar to that described in the work of Luan et al.,[49] which deals with the alumination of mesoporous SBA-15 molecular sieve material. In brief, alumination of MCM-48 was performed by mixing 1.0 g of siliceous MCM-48 into 50 mL of water that contained 137 mg of sodium aluminate (Si/Al = 10) at room temperature for 24 h. The resultant mixture was then centrifuged, washed with distilled water, dried at 313 K in air, and then calcined in static air at 773 K for 5 h. The final granulated powder is designated AlMCM-48.

B. Formation of the H-Aggregated Thionine/AlMCM-48 Composite. A typical preparation of a thionine/AlMCM-48 composite involved stirring a mixture of 500 mg of AlMCM-48 in 15 mL of monomeric thionine solution (derived from 5.0 mg of thionine dye dissolved in 15 mL of water) for at least 24 h at room temperature. The suspension was then centrifuged and the transparent aqueous solution decanted. The residue was washed at least three times with distilled water to remove thionine molecules from the external surface. The product is herein designed thionine/AlMCM-48.

C. Quantum Chemical Structure and Vibrational Frequencies Calculation Methods. The ground state geometry of the thionine cation was optimized without restriction on the symmetry of the initial structure. Both structure optimization and vibrational analysis calculations were implemented by using density functional theory (DFT) with functionals,[47] specifically, B3LYP, in which the exchange functional is of the Becke's three parameter type, including gradient correction, and the correlation correction (see ref 50) involved the gradient-corrected functional of Lee, Yang, and Parr.[51] The split valence type basis sets 6-31G(d,p) and 6-31+G(d,p),[52] as contained in the Gaussian 98 software package,[53] were used.

The vibrational mode descriptions were made through association of measured Raman band positions and intensities with calculated vibrational frequencies and relative intensities, combined with visual inspection of animated normal modes, to assess which bond and angle motions dominate the mode dynamics for the molecule. The DFT method was chosen because we have

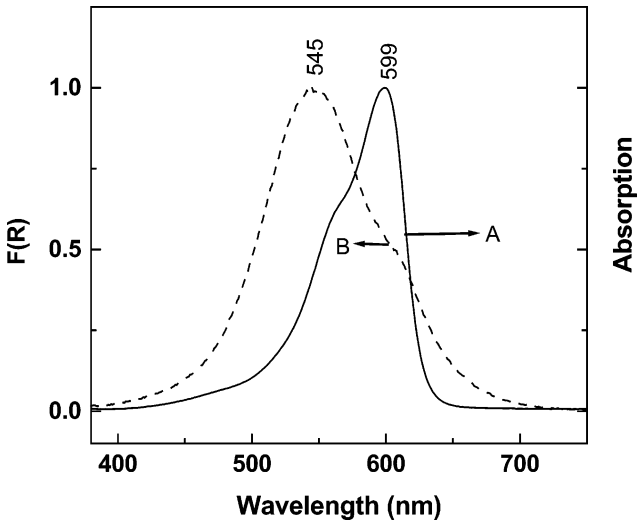

Figure 2. UV−vis spectra of thionine in various environments. (A) Homogeneous solution phase monomeric thionine at 1×10^{-4} M in water solvent (solid line). (B) H-aggregated thionine/AlMCM-48 composite (dashed line).

found it to be computationally less demanding than other theoretical approaches as regards inclusion of electron correlation. For future studies and expansions of the present effort, we shall apply principal component analysis (PCA) methods to provide a more objective means of ascertaining which vibrational modes are associated with specific Raman bands.[54,55]

D. Instrumentation. Absorption spectra were recorded using a Perkin-Elmer Lambda 18 UV−vis−NIR spectrometer. Steady-state fluorescence and excitation spectra were acquired using a SPEX Fluorolog-τ2 spectrofluorometer. Raman spectra were excited with incident radiation of wavelength 457.9 nm provided by a Coherent Innova 200 argon-ion laser; the excitation power was maintained at 120 mW at the laser head, and the Raman scattered radiation was collected and dispersed by a Spex 1877, 0.6-m spectrometer. A Spex Spectrum-1 CCD camera (maintained at 140 K by liquid nitrogen) coupled to the Spex 1877 was used as the detector. The X-ray diffraction (XRD) instrument used was a Rigaku diffractometer, using Cu Kα1 (0.154 nm) X-rays: typically run at a voltage of 40 kV and current of 30 mA.

III. Results and Discussion

XRD patterns of calcined siliceous MCM-48, aluminum-containing AlMCM-48, and the aggregate-incorporated composite, thionine/AlMCM-48, are shown in Figure 1. The pattern for calcined MCM-48 (see Figure 1, curve A) consists of several indexable Bragg peaks. For both aluminum-containing AlMCM-48 and the aggregate-incorporated composite, the XRD patterns have strong (211) and (220) peaks, similar to the case of the MCM-48 parent structure, but the (420) and (332) peaks are not discernible (see Figure 1, curves B and C, respectively). The X-ray measurements are interpreted as indicating that the structural integrity of both AlMCM-48 and the composite material are retained despite alumination and incorporation of thionine dye within the cubic cages. Moreover, nitrogen adsorption−desorption isotherm measurements have been conducted and indicate that the AlMCM-48 that we synthesized has a pore size distribution with one major peak at circa 27 Å (see the Supporting Information).[45]

The diffuse reflectance (DR) UV−vis spectrum of a thionine/AlMCM-48 composite sample is shown in Figure 2 (curve B). The absorption band maximum occurs at 545 nm. Also shown in Figure 2 (curve A), for comparison purposes, is the transmission UV−vis spectrum of aqueous phase thionine, where the absorption band at 599 nm indicates the existence of monomeric thionine. The blue shift in the absorption band upon encapsulating thionine within AlMCM-48, as referenced to the monomer in solution, is attributable to the existence of an aggregate structure for the dye, appropriately termed an H-aggregate, due to the likely alignment of several molecules along the pore axis of AlMCM-48. The broadness of the H-band suggests the existence of sites with different interaction strengths that interact with the occluded aggregate, that is, site-specific perturbations (leading to different lengths of the aggregate or different levels of hydration), as has been postulated for an encapsulated cyanine dye that has been studied in this laboratory.[38]

Our present study has shown that H-aggregates do not form within the one-dimensional channels of aluminum-containing MCM-41 (i.e., AlMCM-41) with pore size of circa 24 Å (not shown); rather, only the monomer exists. This latter finding indicates that the size of the cubic pore structure of AlMCM-48 plays a key role in the formation of H-aggregates, as was also found for thionine in Y zeolite (pore dimension ca. 12 Å).[43] Which suggests that the transverse cross section of thionine must lie effectively perpendicular to the pore axis in order for the H-aggregate to form, explaining why such an orientation may be facilitated for AlMCM-48 but not for AlMCM-41. Additionally, we have found that drying our thionine/AlMCM-48 composite resulted in a change of color indicating formation of monomeric species, as was also found for thionine in Y zeolite.[43] Consequently, we deduce that thionine dye molecules within the pores of AlMCM-48 experience H-bonding when water is present, as well as the typical electrostatic and dipolar forces that lead to aggregates in a wide range of environments. The electrostatic forces between chromophores are expected to be diminished by counterions, thus suggesting that hydrogen bonding and dipolar interactions would result in an alignment of thionines that is similar to that when it is encapsulated in Y zeolite. The extended channels of AlMCM-48 compared to those of Y zeolite, however, would be expected to allow a greater number of molecules to participate in a side-by-side alignment (of π-type orbitals) in the physical aggregate and to correspond, as a result, to the traditional definition of an H-aggregate, with a larger blue shift in the aggregate absorption band relative to that reported for thionine in Y zeolite (i.e., 545 vs 560 nm, respectively).[43] The larger shift, of course, signals the participation of a larger number of monomers in any collective optical process, that is, an increase in the so-called coherence length.

Fluorescence spectra, at two different excitation wavelengths, for solution phase thionine and for a suspension of the composite were also acquired (see Figure 3). As shown in plots A and B of Figure 3, which were acquired with excitation at 580 and 545 nm, respectively, the emissions from thionine in solution are essentially identical (and strong) for the two excitation wavelengths; that is, for both excitation wavelengths, a strong band with a peak at circa 620 nm with a vibronic shoulder extending to the red is evidenced. These spectra correspond to that of the monomer. For the composite system, however, only extremely weak fluorescence, for a range of excitation wavelengths, were found. Curves C and D of Figure 3 show resultant signals for excitation wavelengths of 580 and 545 nm, respectively. The weak fluorescence for the composite system is consistent with the fact that H-aggregates are known to be have a small cross section for fluorescence, resulting from the forbidden character of the dipolar transition between the lowest excited singlet and ground singlet states.[43,44] The weak fluo-

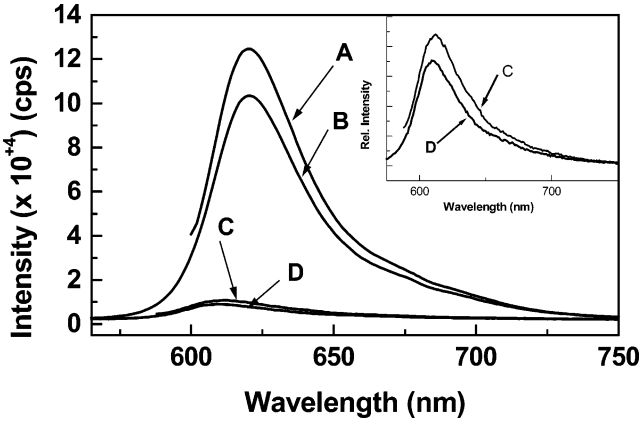

Figure 3. Fluorescence spectra of homogeneous solution phase monomeric thionine of concentration 1×10^{-4} M in water: (A) $\lambda_{ex} =$ 580 nm, and (B) $\lambda_{ex} = 545$ nm. Also, fluorescence spectra of an aqueous suspension of the composite (thionine/AlMCM-48): (C) $\lambda_{ex} = 580$ nm, and (D) $\lambda_{ex} = 545$ nm.

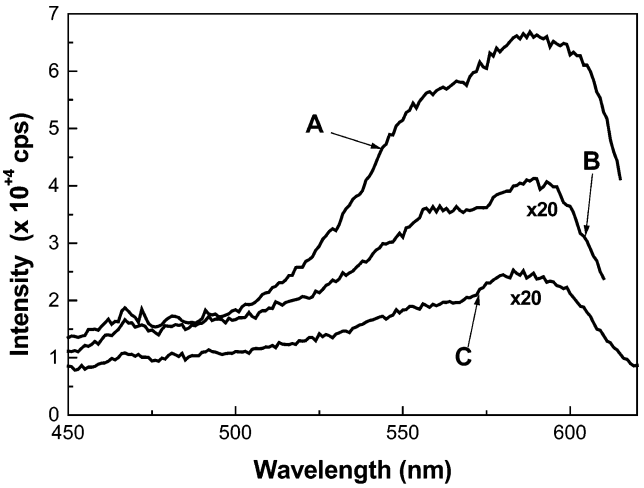

Figure 4. Excitation spectra of homogeneous solution phase monomeric thionine of concentration 1×10^{-4} M in water (curve A), the composite (thionine/AlMCM-48) with the detection wavelength set at 620 nm (curve B), and the composite (thionine/AlMCM-48) with the detection wavelength set at 640 nm (curve C). Intensities of curves B and C have been multiplied by a factor of 20.

rescence is attributable to some small portion of thionine dye which exists in the form of monomer while the majority of dye is in the form of H-aggregated molecules. To confirm the above conclusion, the excitation spectra for solution phase thionine and for a suspension of the composite were also acquired (Figure 4). As shown in Figure 4, the band position and band shape of excitation spectra for the two samples, the former with detection wavelength of 620 nm and the latter measured with detection wavelengths of 620 nm (curve B) and 640 nm (curve C), are essentially identical and mimic the absorption spectrum of solution phase monomer thionine (curve A), indicating that the fluorescence of both samples originated from thionine monomer.

Raman spectra of solution phase thionine and the composite consisting of aggregated thionine encapsulated within AlMCM-48, both excited using 457.9 nm radiation, are shown in Figure 5 (curves A and B, respectively). The observed peak positions for the Raman bands of solution phase thionine found in the present study and those of polycrystalline thionine, as reported by Hutchinson et al.,[46] are found to be almost identical.

As regards band assignments, Hutchinson et al. provided approximate attributions of bands to specific vibrational motions between atoms in the thionine molecule.[46] However, their

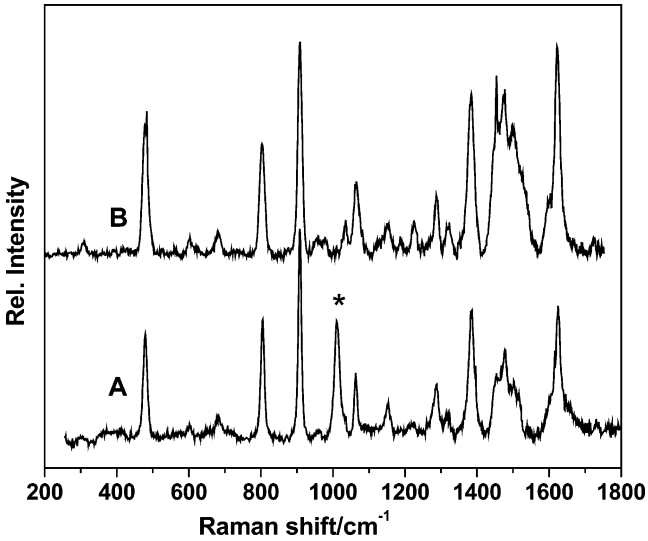

Figure 5. Raman spectra of (A) homogeneous solution phase monomeric thionine at 1×10^{-4} M in water/methanol solvent with excitation wavelength = 457.9 nm; (B) H-aggregated thionine AlMCM-48 composite, excitation wavelength = 457.9 nm. The asterisk labels a solvent Raman band.

assignments were extremely limited. Here we report the assignment of the calculated vibrational modes of gas phase thionine based on the density functional prediction. The calculated frequencies agree very closely with the observed Raman band frequencies for the solution phase system without the imposition of a scaling factor (see Table 1). Moreover, through the use of animation software, we determined which nuclear motions principally contribute to a particular normal mode, also shown in Table 1. We found, based on such studies, that all nuclear motions are in-plane. Figure 6 shows some of the selected vibrational mode motions for the ground state structure of the thionine cation molecule. It is also observed that the patterns of Raman spectra for both solution thionine monomer and thionine H-aggregate in the composite system are very similar, especially as regards band positions. We deduce that although thionine H-aggregate is formed within AlMCM-48, the molecular structure of thionine, to a high degree, is independent of its environment.

The observed Raman spectra of the monomer and aggregated thionine cation with assignment of these vibrational modes of the frequencies based on the B3LYP calculation, including charge distribution within thionine molecules and components of the calculated dipole moments, suggests that thionine monomers in the aggregate overlap via face-to-face packing. This is in agreement with $\pi-\pi^*$ interactions between aromatic chromophores that often play a dominant role in holding molecules together within an aggregate.

IV. Conclusion

The combination of XRD, UV−vis absorption, fluorescence, and Raman measurements of thionine in solution and AlMCM-48 indicates that we are able to form H-aggregated thionine occluded in the core. The aggregates within the mesoporous AlMCM-48 probably involve more than two or three monomers in the physical aggregate, and it is more appropriately termed an H-aggregate. We have deduced that the transverse cross section of thionine, when the H-aggregate is formed, must lie effectively perpendicular to the pore axis, resulting in a side-by-side alignment (of π-type orbitals) of thionine monomers in the physical aggregate. The vibrational modes in the Raman

TABLE 1: Assignment of Raman Bands of Monomeric and Aggregated Thionine

symmetry	calc(int)	solution meas(int)	composite	assignment[a]
A′	311(0.09)	318(0.17)	313(0.46)	T($Q_{1,3}$ and NH_2) and $\delta(Q_2)$ due to the bending vibration of the C−S−C bond.
A′	436(0.16)	441(0.14)	437(0.12)	Asymmetric skeletal deformation of the rings Q_{1-3} due to the ν_{as}(C−S−C) and stretching of the ring 1,3 along the C_4↔C_8/$C_{4'}$↔$C_{8'}$ direction in opposing phases.
A′	484(0.11)	486(0.96)	484(1.41)	R($Q_{1,3}$) and stretching of the ring Q_2 along the S↔N direction, accompanied by $\rho(NH_2)$.
A′	616(0.01)	610(0.15)	607(0.20)	Skeletal deformation resulting from δ(C−S−C)/δ(C−C_3−C)/δ(C−$C_{3'}$−C)
A′	694(0.05)	687(0.14)	688(0.23)	Skeletal deformation caused by breathing of the ring Q_2 and stretching of the ring $Q_{1,3}$ along the short molecular axis direction.
A′	813(0.01)	812(1.00)	810(1.00)	Asymmetric skeletal deformation due to the δ(C−N−C)/δ(C−S−C)/δ(C−C−C) and stretching of the HN−C, ν(HN−C).
A′	923(0.08)	906(1.72)	964(0.13)	Skeletal deformation resulting from the ν(C−S−C) and stretching of the ring $Q_{1,3}$ along the C_4↔C_8 and $C_{4'}$↔$C_{8'}$ direction, respectively; accompanied by ν(HN−C) and in-plane wagging of C_5H and $C_{5'}$H.
A′	1045(0.004)	1041(0.15)	1042(0.33)	Asymmetric skeletal deformation due to the ν_{as}(C−S−C)/δ(C−C−C) and w(CH)/w(NH_2).
A′	1063(1)		1072(0.61)	w(NH_2)/w(C_2H and $C_{2'}$H).
A′	1082(0.05)	1070(0.53)	1157(0.40)	Asymmetric skeletal deformation of the rings $Q_{1,3}$ due to the δ(C−C_7−C)/δ(C−$C_{7'}$−C) and symmetric skeletal deformation of the ring Q_3 caused by ν(C−S−C); accompanied by w(NH_2)/β(C_2H and $C_{2'}$H) and CH bonds waggings, w(CH).
A′	1165(0.01)	1152	1232(0.32)	w(C_nH), n = 4, 5, 4′, and 5′.
A′	1290(0.01)	1293(0.39)	1294(0.50)	Skeletal deformation caused by δ(C−N−C); accompanied by β(C_nH), n = 2, 5, 2′, and 5′.
A′	1323(0.01)	1328(0.10)	1326(0.25)	Half-ring-skeletal deformation due to ν(CNC)/δ(CCC); accompanied by ν(HN−C)/β(CH).
A′	1390(0.62)	1391(1.39)	1391(1.45)	Skeletal deformation resulting from ν(C−C); accompanied by ν(HN−C) and β(NH_{13} and $NH_{13'}$)/β(C_nH), n = 4, 5, 4′, and 5′.
A′	1496(0.02)	1463(0.06)	1481(1.43)	Asymmetric skeletal deformation due to the ν(C−C−C)/ν(C−C−C) and ν_{as}(C−N−C); accompanied by β(H−N−C)/β(C_2H and $C_{2'}$H).
A′	1510(0.31)	1485(1.10)	1505(0.13)	Asymmetric skeletal deformation due to the ν(C_2−C_8)/ν($C_{2'}$−$C_{8'}$) and (C_4−C_5)/($C_{4'}$−$C_{5'}$) (in opposing phases) and δ(C−N−C); accompanied by β(NH_{14} and $NH_{14'}$)/β(C_nH), n = 2, 4, 2′, and 4′.
A′	1535(0.07)	1511(0.99)		Asymmetric skeletal deformation due to the ν_{as}(C−C_2−C)/ν_{as}(C−$C_{2'}$−C) and ν(C_7−C_8)/ν($C_{7'}$−$C_{8'}$); accompanied by β(H−N−C), including β(C_nH), n = 2 and 2′.
A′	1670(0.15)	1631(1.64)	1629(1.72)	NH_2 scissoring; accompanied by weak $\delta(Q_{1\text{ and }2})$ due to the ν($C_4$$C_5$)/$\nu$($C_{4'}$$C_{5'}$), combined by relatively weak in-plane bending of CH bonds, β(CH).

[a] The parameters used here: Q_1, Q_2, and Q_3 are the three rings in thionine, with 1 and 3 referring to the outer ring systems; T, translation; R, rotation; ν, stretch; δ, skeletal deformation; β, bending deformation; ρ, rocking motion; w, wagging.

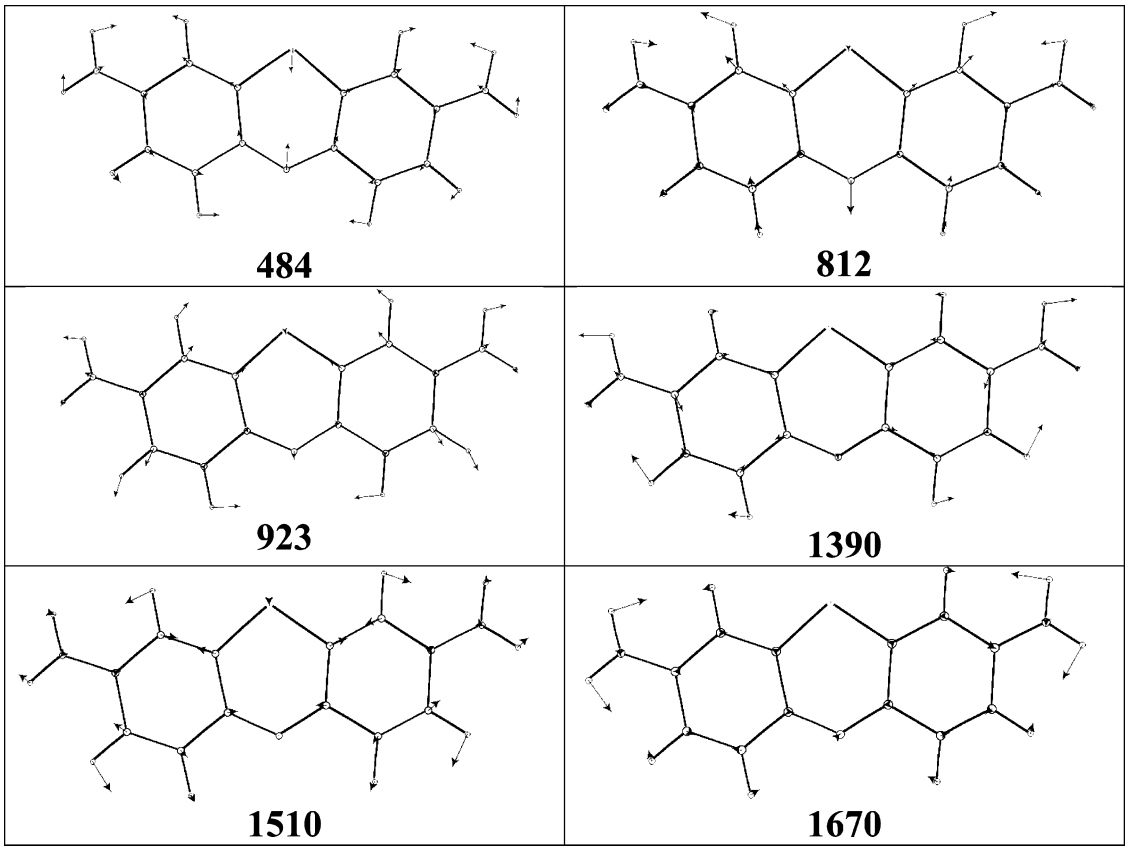

Figure 6. Selected vibrational modes of the ground state thionine cationic molecule.

spectrum of aggregated thionine are closely approximated in terms of frequency and relative intensity by calculations based on density functional methods at the B3LYP level.

It is to be noted that the nonfluorescing nature of the H-aggregated form is anticipated as promoting formation of triplet state species, which might effectively transfer energy to lower triplet species and, as suggested in the literature,[44] serve to harvest radiation in a solar energy conversion system. In particular, the mesoporous structure of AlMCM-48 makes it possible to encapsulate energy acceptors, such as phenanthrene and 1-methylnaphalene, within the same cubic pore, which would serve to funnel energy to an appropriate receptor. We

are presently conducting detailed studies on energy transfer from H-aggregate to acceptors.

Acknowledgment. D.L.A. thanks the NSF and DoD-ARO for support of this work, in part, through the following awards: (1) NSF-IGERT program under Grant DGE-9972892, (2) NSF-MRSEC program under Grant DMR-0213574, and (3) DoD-ARO under Cooperative Agreement DAAD19-01-1-0759. Also, we thank Dr. Maria C. Tamargo, a colleague at CCNY, for use of her Rigaku X-ray diffractometer.

Supporting Information Available: Pore size distribution in synthesized AlMCM-46. This material is available free of charge via the Internet at http://pubs.acs.org.

References and Notes

(1) Akins, D. L.; Özçelik, S.; Zhu, H.-R.; Guo, C. *J. Phys. Chem. A* **1997**, *101*, 3251.
(2) Özçelik, S.; Akins, D. L. *J. Phys. Chem. B* **1999**, *103*, 8926.
(3) Akins, D. L. *J. Phys. Chem.* **1986**, *90*, 1530.
(4) Akins, D. L. *J. Colloid Interface Sci.* **1982**, *90*, 373.
(5) Li, X.; Gu, B.; Akins, D. L. *Chem. Phys. Lett.* **1984**, *105*, 263.
(6) Gu, B.; Akins, D. L. *Chem. Phys. Lett.* **1985**, *113*, 558.
(7) Akins, D. L.; Akpabli, C.; Li, X. *J. Phys. Chem.* **1989**, *93*, 1977.
(8) Akins, D. L.; Macklin, J. W. *J. Phys. Chem.* **1989**, *93*, 5999.
(9) Akins, D. L.; Macklin, J. W.; Parker, L.; Zhu, H.-R. *Chem. Phys. Lett.* **1990**, *169*, 564.
(10) Akins, D. L.; Macklin, J. W.; Zhu, H.-R. *J. Phys. Chem.* **1990**, *95*, 793.
(11) Akins, D. L.; Zhu, H.-R. *Langmuir* **1992**, *8*, 546.
(12) Akins, D. L.; Macklin, J. W.; Zhu, H.-R. *J. Phys. Chem.* **1992**, *96*, 4515.
(13) Akins, D. L.; Zhuang, Y. H.; Zhu, H.-R.; Li, J. Q. *J. Phys. Chem.* **1993**, *98*, 1068.
(14) Akins, D. L. In *J-Aggregate*; Kobayashi, T., Ed.; World Scientific: Singapore, 1996; pp 67−94.
(15) Gilman, P. B. *Photogr. Sci. Eng.* **1974**, *18*, 418.
(16) Hanamura, E. *Phys. Rev. B* **1988**, *37*, 1273.
(17) Sasaki, F.; Kobayashi, S. *Appl. Phys. Lett.* **1993**, *63*, 2887.
(18) Wang, Y. *Chem. Phys. Lett.* **1986**, *126*, 209.
(19) Wang, Y. *J. Opt. Soc. Am. B* **1991**, *8*, 981.
(20) Kobayashi, S. *Mol. Cryst. Liq. Cryst.* **1992**, *217*, 77.
(21) Kasha, M. *Radiat. Res.* **1963**, *20*, 55.
(22) Sturmer, D. M.; Heseltine, D. W. In *The Theory of the Photographic Process*, 4th ed.; James, T. H., Ed.; MacMillian Publishing Co.: New York, 1977; Chapter 8.
(23) Herz, A. H. *Adv. Colloid Interface Sci.* **1977**, *8*, 237.
(24) Mobius, D.; Kuhn, H. *Isr. J. Chem.* **1979**, *18*, 375.
(25) Mobius, D. *Acc. Chem. Res.* **1981**, *14*, 63.
(26) Akins, D. L. *J. Phys. Chem.* **1986**, *90*, 1530.
(27) Akins, D. L.; Lombardi, J. R. *Chem. Phys. Lett.* **1987**, *136*, 495.
(28) Selwyn, J. E.; Steinfeld, J. I. *J. Phys. Chem.* **1972**, *76*, 762.
(29) Ojeda, P. R.; Amashta, I. A. K.; Ochoa, J. R.; Arbeloa, I. L. *J. Chem. Soc., Faraday Trans. 2* **1988**, *84*, 1.
(30) Valdes-Aguilera, O.; Neckers, D. C. *Acc. Chem. Res.* **1989**, *22*, 171.
(31) Steinhurst, D. A.; Baronavski, A. P.; Owrutsky, J. C. *J. Phys. Chem. B* **2002**, *106*, 3160.
(32) Kasha, M.; Rawls, H. R.; El-Bayoumi, M. A. *Pure Appl. Chem.* **1965**, *11*, 37.
(33) Hessemann, J. *J. Am. Chem. Soc.* **1980**, *102*, 2167, 2176.
(34) Vincent, P. S.; Barlow, W. A. *Thin Solid Films* **1980**, *71*, 305.
(35) Fukuda, K.; Nakahara, H. *J. Colloid Interface Sci.* **1984**, *98*, 555.
(36) Mooney, W. F.; Brown, P. E.; Russel, J. C.; Costa, S. B.; Pederson, L. G.; Whitten, D. G. *J. Am. Chem. Soc.* **1984**, *106*, 5659.
(37) Mooney, W. F.; Whitten, D. G. *J. Am. Chem. Soc.* **1986**, *108*, 5712.
(38) Xu, W.; Guo, H.; Akins, D. L. *J. Phys. Chem. B* **2001**, *105*, 1543.
(39) Akins, D. L.; Zhu, H.-R.; Guo, C. *J. Phys. Chem.* **1994**, *98*, 3612.
(40) Akins, D. L.; Zhu, H.-R.; Guo, C. *J. Phys. Chem.* **1996**, *100*, 5420.
(41) Guo, C.; Ren, B.; Akins, D. L. *J. Phys. Chem. B* **1998**, *102*, 8751.
(42) Calzaferri, G.; Huber, S.; Dobler, J.; Maas, H.; Minkowski, C. *Angew Chem. Int. Ed.* **2003**, *42* (32), 3732.
(43) Ramamurthy, V.; Sanderson, D. R.; Eaton, D. F. *J. Am. Chem. Soc.* **1993**, *115*, 10438
(44) Das, S.; Kamat, P. V. *J. Phys. Chem. B* **1999**, *103*, 209.
(45) The pore size of MCM-48 was 27 Å, as determined through nitrogen adsorption/desorption as indicated in the Supporting Information.
(46) Hutchinson, K.; Hester, R. E.; Albery, W. J.; Hillman A. R. *J. Chem. Soc., Faraday Trans. 1* **1984**, *80*, 2053.
(47) Bartolotti, L. J.; Flurchick. In *Review in Computational Chemistry*; Lipkowitz, K. B., Boyd, D. B., Eds.; VCH Publishers Inc.: New York, 1996; Vol. 7, Chapter 4.
(48) Thommes, M.; Köhn, R.; Fröba, M. *J. Phys. Chem. B* **2000**, *104*, 7932.
(49) Luan, Z.; Hartmann, M.; Zhao, D.; Zhou, W.; Kevan, L. *Chem. Mater.* **1999**, *11*, 1621.
(50) Becke, A. D. *Phys. Rev. A* **1988**, *38*, 3098.
(51) Lee, C.; Yang, W.; Parr, R. G. *Phys. Rev. B* **1993**, *37*, 785.
(52) Gordon, M. S. *Chem. Phys. Lett.* **1980**, *76*, 163.
(53) Frisch, M. J.; Trucks, G. W.; Schlegel, H. B.; Scuseria, G. E.; Robb, M. A.; Cheeseman, J. R.; Zakrzewski, V. G.; Montgomery, J. A., Jr.; Stratmann, R. E.; Burant, J. C.; Dapprich, S.; Millam, J. M.; Daniels, A. D.; Kudin, K. N.; Strain, M. C.; Farkas, O.; Tomasi, J.; Barone, V.; Cossi, M.; Cammi, R.; Mennucci, B.; Pomelli, C.; Adamo, C.; Clifford, S.; Ochterski, J.; Petersson, G. A.; Ayala, P. Y.; Cui, Q.; Morokuma, K.; Malick, D. K.; Rabuck, A. D.; Raghavachari, K.; Foresman, J. B.; Cioslowski, J.; Ortiz, J. V.; Stefanov, B. B.; Liu, G.; Liashenko, A.; Piskorz, P.; Komaromi, I.; Gomperts, R.; Martin, R. L.; Fox, D. J.; Keith, T.; Al-Laham, M. A.; Peng, C. Y.; Nanayakkara, A.; Gonzalez, C.; Challacombe, M.; Gill, P. M. W.; Johnson, B. G.; Chen, W.; Wong, M. W.; Andres, J. L.; Head-Gordon, M.; Replogle, E. S.; Pople, J. A. *Gaussian 98*, revision A.7; Gaussian, Inc.: Pittsburgh, PA, 1998.
(54) Wheeler, R. A.; Dong, H. T.; Boesch, S. E. *Chem. Phys. Chem.* **2003**, *4*, 382.
(55) Wheeler, R. A.; Dong, H. T. *Chem. Phys. Chem.* **2003**, *4*, 1227.